

On the instability of the flow in an oscillating tank of fluid

By PHILIP HALL

Department of Mathematics, University of Manchester, Manchester M13 9PL, UK

(Received 9 February 1993 and in revised form 1 November 1993)

The instability of a viscous fluid inside a rectangular tank oscillating about an axis parallel to the largest face of the tank is investigated in the linear regime. The flow is shown to be unstable to both longitudinal roll and standing wave instabilities. The particular cases of low and high oscillation frequencies are discussed in detail. The relationship between the roll instability and convective or centrifugal instabilities in unsteady boundary layers is discussed. The eigenvalue problems associated with the roll and standing wave instabilities are solved using Floquet theory and a combination of numerical and asymptotic methods. The results obtained are compared to the recent experimental investigation of Bolton & Maurer (1994) which indeed provided the stimulus for the present investigation.

1. Introduction

Our concern is with the instability of the unsteady flow of a viscous fluid inside a rectangular tank oscillating about an axis parallel to one face of the tank. The orientation of the axis of oscillation is shown in figure 1 of Bolton & Maurer (1994). An experimental investigation of the different regimes for the flow inside the tank is described in Bolton & Maurer (1994), hereafter referred to as BM). If the geometry of the tank is such that

$$L_x/d, L_y/d \gg 1$$

then near the axis the basic flow is unidirectional (in the x^* direction) and dependent only on y^* and time. In fact the flow is an exact solution of the Navier–Stokes equations. The stability of the flow is therefore governed by a system of partial differential equations with coefficients periodic in time. We shall show that the linear instability problem is closely related to those for centrifugal and convective instabilities in time-periodic flows. Before discussing the results of BM we shall first briefly review the relevant details of the related flows mentioned above.

The experimental and theoretical investigations of the centrifugal instability of a Stokes layer by Seminara & Hall (1976) showed that time-periodic flows can sustain instabilities not accessible to quasi-steady instability theories based on the instantaneous velocity profiles. Seminara & Hall (1976) found that a torsionally oscillating cylinder in a viscous fluid drives an unsteady boundary layer which is unstable to Taylor-vortex-like instabilities at high enough frequencies of oscillation. A more detailed experimental investigation of the problem by Park, Barenghi & Donnelly (1980) confirmed the secondary subharmonic destabilization of the most dangerous mode found by Seminara & Hall (1976). An approximate description of this subharmonic breakdown was later given by Hall (1981). Subsequently it was shown by Hall (1984) and Papageorgiou (1987) that the instability mechanism found by

Seminara & Hall can occur in spatially localized positions in more complicated unsteady boundary-layer flows.

The convection mode of instability of the unsteady thermal boundary layer in a semi-infinite mass of fluid adjacent to a time-periodically heated rigid wall was investigated theoretically by Hall (1985). In the latter paper it was shown that the convection problem for a fluid with Prandtl number equal to unity is identical to that governing the centrifugal instability problem for the flow adjacent to a rapidly rotating cylinder in a uniform stream. As yet only the severely truncated equations discussed by Hall have been solved and the results found suggest that the most dangerous mode is a subharmonic one. If that is the only unstable mode then Hall's analysis suggests that the flow outside a rapidly rotating cylinder is stable since in that problem the polar angle θ plays the role of time and solutions periodic in θ with period 4π are of no physical relevance.

Another convection problem associated with time-periodic forcing is that discussed by Gresho & Sani (1970), who investigated the instability of a layer of fluid heated steadily from below in a time-periodic gravity field. It was found that the stability problem is governed by Mathieu's equation and that the dominant instability is a subharmonic one. The problem discussed by Gresho & Sani is of considerable practical importance because of the presence of convection in a micro-gravity environment where vibrations cause the effective gravitational field to be oscillatory in time.

The possible instability of time-periodic flows to travelling wave disturbances has by contrast not received much attention. One of the fundamental problems here concerns the linear instability of a Stokes layer on a transversely oscillating rigid plane wall to waves propagating in the flow direction. This problem was first investigated by Kerczek & Davis (1974) who found that, even though the instantaneous profiles can be highly inflexional and therefore unstable, the oscillatory flow between parallel plates is stable according to a Floquet approach. Later Hall (1978) showed that, even though the Floquet solutions of Kerczek & Davis were greatly dependent on the presence of a stationary wall, the Stokes layer on a wall oscillating in a viscous fluid is stable. However, the instantaneous velocity profiles associated with a Stokes layer can be unstable on the basis of a quasi-steady analysis. Such an approach is valid at large Reynolds numbers; however, the unstable solutions cannot be continued over a full period of oscillation to produce Floquet solutions. More recent work by Akhavan, Kamm & Shapiro (1991 *a, b*), based on full numerical simulations of the Navier–Stokes equations, suggests that transition to turbulence in Stokes layers can be attributed to higher-order instabilities associated with the primary instabilities of the instantaneously inviscidly unstable velocity profile of the basic state.

We shall now discuss the main results found by BM in their experimental investigation of the flow in a flapping rectangular tank. A more detailed discussion of the results can be found in BM.

In order to characterize the frequency of the flow BM introduced the parameter $\Phi = \omega d^2/\nu$, where ω is the frequency of oscillation, ν the kinematic viscosity and d the width of the tank. At a fixed value of the flapping angle α BM observed that at small enough values of Φ the flow was stable. When Φ was increased a bifurcation to a weak roll state took place at a critical value of Φ . If this critical value of Φ is denoted by Φ_{c1} then BM showed that Φ_{c1} is a monotonically decreasing function of α . At a second critical value of α , Φ_{c2} , a strong roll state was found by BM and at sufficiently small values of α this mode exhibited hysteresis. At higher values of Φ wavy modes were observed experimentally though BM suggest that these modes are dependent on the roll wavelength, which is quantized by the vertical length of the container. At very high

values of Φ a turbulent flow superimposed on some residual roll structure was observed in the experiments. The analysis in this paper will focus on the origin of the strong vortex state found experimentally; however, our results will also suggest a likely candidate for a mode responsible for the onset of the wavy states.

In the following section we shall formulate the linear instability problem for the unidirectional flow in an infinitely long flapping tank. The equations we derive govern the linear instability of the flow to disturbances periodic in the x^* and z^* directions. In §3 these equations are discussed for roll modes which are taken to be independent of x^* . The particular cases of large and small Φ are discussed in §3 whilst in §4 numerical results for Φ of $O(1)$ size are presented and our results compared to experimental observations. In §5 we discuss travelling wave disturbances which are independent of z^* . Finally in §5 we draw some conclusions.

2. Basic flow and the stability problem

Consider the flow of a viscous fluid in the rectangular container defined by

$$-L_x < x^* < L_x, \quad -\frac{1}{2}d < y^* < \frac{1}{2}d, \quad -L_z < z^* < L_z \quad (2.1)$$

with respect to a Cartesian coordinate system (x^*, y^*, z^*) . The fluid is taken to be incompressible and the density and viscosity are denoted by ρ and ν respectively. The fluid is set in motion by the oscillation of the container about the z^* axis with angular velocity $(0, 0, \alpha\omega \sin \omega t^*)$. Following BM we define the frequency parameter Φ by

$$\Phi = \omega d^2 / \nu \quad (2.2)$$

so that $\Phi \gg 1$ corresponds to a situation where viscous effects are small whilst $\Phi \ll 1$ corresponds to a viscous-dominated flow. We can suppose that the velocity and pressure of the fluid are scaled on $\alpha\omega d$ and $\alpha\rho\omega^2 d^2$ respectively whilst dimensionless variables (x, y, z) and t are defined by

$$(x, y, z) = d^{-1}(x^*, y^*, z^*), \quad t = \omega t^*, \quad (2.3)$$

where t^* denotes time. With respect to the coordinate system moving with the tank the Navier–Stokes equations take the form

$$\nabla \cdot \mathbf{u} = 0,$$

$$\mathbf{u}_t + \alpha(\mathbf{u} \cdot \nabla) \mathbf{u} - \frac{1}{\Phi} \Delta \mathbf{u} = -\nabla p + 2\alpha \sin t \begin{pmatrix} v \\ -u \\ 0 \end{pmatrix} + \alpha \sin^2 t \begin{pmatrix} x \\ y \\ 0 \end{pmatrix} + \cos t \begin{pmatrix} y \\ -x \\ 0 \end{pmatrix}, \quad (2.4)$$

where subscripts denote partial derivatives.

The above equations must be solved subject to

$$\mathbf{u} = 0 \quad \text{on} \quad x = \pm L_x/d, \quad y = \pm \frac{1}{2}, \quad z = \pm L_z/d. \quad (2.5)$$

If we write

$$p = \frac{1}{2}\alpha \sin^2 t (x^2 + y^2) - xy \cos t + \hat{p}$$

then (2.4) becomes

$$\mathbf{u}_t + \alpha(\mathbf{u} \cdot \nabla) \mathbf{u} - \frac{1}{\Phi} \Delta \mathbf{u} = -\nabla \hat{p} + 2\alpha \sin t \begin{pmatrix} v \\ -u \\ 0 \end{pmatrix} + \begin{pmatrix} 2y \cos t \\ 0 \\ 0 \end{pmatrix}, \quad (2.6)$$

and for convenience we now drop the \wedge notation.

In order to make analytical progress we assume that $L_x/d, L_z/d$ are large so that we can drop the boundary conditions at $x = \pm L_x/d, z = \pm L_z/d$. As in BM this enables us to look for a unidirectional flow of the form

$$\mathbf{u} = (\bar{u}(y, t), 0, 0), \quad v = w = 0, \quad p = -2\alpha \sin t \int^y u \, dy,$$

where
$$\left. \begin{aligned} -(1/\Phi) \bar{u}_{yy} + \bar{u}_t &= 2y \cos t, \\ \bar{u} &= 0, \quad y = \pm \frac{1}{2}. \end{aligned} \right\} \tag{2.7}$$

The required solution is

$$\bar{u} = \{-yi + Q\} e^{it} + \text{complex conjugate}, \tag{2.8}$$

where
$$Q = \frac{i \sinh [(i\Phi)^{\frac{1}{2}} y]}{2 \sinh [(i\Phi)^{\frac{1}{2}} \frac{1}{2}]}. \tag{2.9}$$

(Note that $\bar{u} = U/\alpha\omega d$ in the notation of BM.) For large values of Φ the function Q is exponentially small away from layers of depth $O(\Phi)^{-\frac{1}{2}}$ near $y = \pm \frac{1}{2}$. Thus for large Φ we find that near $y = \frac{1}{2}$

$$\bar{u} = \sin t - \sin [t + (\frac{1}{2}\Phi)^{\frac{1}{2}}(y - \frac{1}{2})] \exp [+ (\frac{1}{2}\Phi)^{\frac{1}{2}}(y - \frac{1}{2})]. \tag{2.10}$$

For small values of Φ the fluid responds in a quasi-steady manner to the forcing and we obtain

$$\bar{u} = \frac{1}{12}\Phi y \{1 - 4y^2\} \cos t + \dots \tag{2.11}$$

At first sight it might appear that the flow in a tank rotating with constant angular velocity is then obtained from the above by setting t equal to zero. However, in the limit $\omega \rightarrow 0$ the parameter Φ also tends to zero so that in the steady limit there is no flow in the tank.

We now perturb the basic flow given by (2.8) by writing

$$\mathbf{u} = (\bar{u}, 0, 0) + [U(y, t) \exp i\{\lambda x + k z\} + \text{complex conjugate}] + \dots \tag{2.12}$$

If we assume that $|U| \ll |\bar{u}|$ then we can linearize (2.6) to give the equation for the Fourier mode with wavenumbers (λ, k) :

$$\left. \begin{aligned} i\lambda U + V_y + ikW &= 0, \\ \mathcal{L}U + \alpha V \bar{u}_y &= -i\lambda P + 2\alpha V \sin t, \\ \mathcal{L}V &= -P_y - 2\alpha U \sin t, \\ \mathcal{L}W &= -ikP. \end{aligned} \right\} \tag{2.13}$$

Here the operator \mathcal{L} is defined by

$$\mathcal{L} = -[\partial_y^2 - \lambda^2 - k^2] \Phi^{-1} + i\alpha \lambda \bar{u} + \partial_t. \tag{2.14}$$

Equations (2.13) must be solved subject to

$$U = V = W = 0, \quad y = \pm \frac{1}{2}. \tag{2.15}$$

Since \bar{u} is a periodic function of time we anticipate that solutions of (2.13) and (2.15) may be found with

$$(U, V, W, P) = e^{\mu t} (\hat{U}, \hat{V}, \hat{W}, \hat{P}) \tag{2.16}$$

where $\hat{U}, \hat{V}, \hat{W}$ and \hat{P} are periodic with respect to t and the Floquet exponent μ is complex and is a function of Φ, α, λ, k . The stability of the flow is then determined by

the sign of μ_r ; if solutions of the form (2.16) exist with $\mu_r > 0$ then the flow is unstable. In the next section we discuss solutions of the eigenvalue problem for the case $\lambda = 0$ which, following BM, we refer to as ‘roll’ modes. In §5 we investigate the possibility of Tollmien–Schlichting wave instabilities.

3. Roll modes of instability

We shall now seek solutions of (2.13) and (2.15) with $\lambda = 0$; it is then convenient to eliminate W and P to give the following coupled pair of equations for U and V :

$$\left. \begin{aligned} (\partial_y^2 - k^2 - \Phi \partial_t) U &= -\alpha \Phi V \{Q_y e^{it} + \bar{Q}_y e^{-it}\}, \\ (\partial_y^2 - k^2 - \Phi \partial_t)(\partial_y^2 - k^2) V &= -2\alpha \Phi k^2 U \sin t, \\ U = V = V_y &= 0, \quad y = \pm \frac{1}{2}. \end{aligned} \right\} \quad (3.1)$$

It is of interest to note that (3.1) also governs the stability of a vertically oscillating Boussinesq fluid between parallel walls $y = \pm \frac{1}{2}$. In that case the fluid has Prandtl number unity and the upper and lower walls have temperature proportional to $\pm \sin t$ respectively, whilst the fluid is subject to a gravitational field proportional to $\sin t$. In that case the Rayleigh number for the flow is $\alpha^2 \Phi^2$ so that at $O(1)$ values of Φ we should anticipate unstable solutions of (3.1) for $\alpha = O(1)$. Before discussing the numerical solution of (3.1) for $O(1)$ values of α and Φ it is instructive for us to first consider the further limits $\Phi \rightarrow 0$ and $\Phi \rightarrow \infty$.

3.1. The low-frequency large-angle limit

In the low-frequency limit (3.1) reduces to

$$\begin{aligned} (\partial_y^2 - k^2 - \Phi \partial_t) U &= -2\alpha \Phi \\ &\times \left\{ \sin t + \Phi \cos t \left[\frac{y^2 - 1}{2} - \frac{1}{24} \right] - \frac{\Phi^2 \sin t}{12} \left(y^4 - \frac{y^2}{2} + \frac{7}{240} \right) \dots \right\} V, \quad (3.2a) \\ (\partial_y^2 - k^2 - \Phi \partial_t)(\partial_y^2 - k^2) V &= -2\alpha \Phi k^2 U \sin t, \quad (3.2b) \\ U = V = V_y &= 0, \quad y = \pm \frac{1}{2}. \quad (3.2c) \end{aligned}$$

We now indicate how a *WKB* type of solution of the above equations can be found. If we set $\alpha = 0$ then the equations for U and V decouple and it is easy to see that the flow is stable with decay rates of size $1/\Phi$ on the t timescale. We anticipate that this decay will then be balanced by growth associated with the apparently destabilizing terms on the right-hand side of (3.2a, b). This is achieved if $\alpha \Phi \sim O(1)$ so that we write

$$\alpha = \frac{A}{\Phi} + \dots$$

and let $(U, V) = (U_0(y), V_0(y)) \exp\{\Phi^{-1} \int^t \sigma dt\} + \dots$. The eigenvalue problem for the local growth rate σ is then found to be given by

$$\left. \begin{aligned} [d_y^2 - k^2 - \sigma] U_0 &= -2A \sin t V_0, \\ [d_y^2 - k^2 - \sigma][d_y^2 - k^2] V_0 &= -2Ak^2 \sin t U_0, \\ U_0 = V_0 = V_{0y} &= 0, \quad y = \pm \frac{1}{2}. \end{aligned} \right\} \quad (3.3)$$

Thus t appears only as a parameter in the zeroth-order problem so we have an ordinary differential system to determine the eigenvalues $\sigma = \sigma(k, A)$. In fact by replacing $V_0 \sin t$ by V_0 we see that (3.3) is then equivalent to the Bénard problem for a fluid of

Prandtl number unity between the plate $y = -\frac{1}{2}$ at temperature unity and the plate $y = \frac{1}{2}$ at zero temperature. However, the effective Rayleigh number is $-4A^2 \sin^2 t$ so that the flow is stable and σ must have a negative real part. This can be seen from (3.3) for large values of A by writing

$$\sigma = \sigma_0 A + \dots, \quad U_0 = U_{00} + \dots, \quad V_0 = V_{00} + \dots \tag{3.4}$$

The eigenvalue problem for σ_0 then becomes

$$\left. \begin{aligned} \sigma_0^2 [d_y^2 - k^2] V_0 &= 4k^2 \sin^2 t V_0, \\ V_0 &= 0, \quad y = \pm \frac{1}{2}. \end{aligned} \right\} \tag{3.5}$$

We notice here that the limit $A \rightarrow \infty$ is an inviscid one so that the eigenvalue problem is now associated with a second-order differential equation. In fact the eigenvalues of (3.5) are

$$\sigma_0 = \pm 2ik(n^2\pi^2 + k^2)^{-\frac{1}{2}} \sin t, \quad n = 1, 2, 3, \dots, \tag{3.6}$$

which means that the flow is inviscidly stable. Thus we have shown above that for $\Phi \gg 1$, $\alpha\Phi \gg 1$ the disturbance has an imaginary growth rate of size $O(\alpha)$.

The above discussion shows that no neutral disturbances exist for $\alpha\Phi = O(1)$, $\Phi \ll 1$. In order to obtain neutral disturbances we must increase α until sufficient exponential growth takes place near the times when $\sin t = 0$ to balance the exponential decay associated with viscous effects at other times. The exponential growth takes place in $O(\Phi)$ time intervals surrounding the times when $\sin t = 0$; this means that in these intervals the disturbance grows by an amount of order $\exp(\alpha C \Phi^2)$ for some constant C . Viscous effects on the other hand lead to decay by factors of size $\exp[(\frac{1}{3}\alpha)^{1/k} D]$ for some D . Thus the decay rate decreases with k if α and Φ are held fixed. However, as we will see later, when k increases to $O(\Phi)^{-\frac{1}{3}}$ viscous effects in the bulk of the flow also come into play and a minimum decay rate is achieved. We therefore seek a solution of (3.2) for the small- Φ case with

$$B = \alpha\Phi^{\frac{1}{3}}, \quad k = K\Phi^{-\frac{1}{3}} \tag{3.7a, b}$$

held fixed. Note here that the scaling $\alpha \sim \Phi^{-\frac{11}{3}}$ enables viscous effects to enter the stability problem at leading order.

We then expand U and V in the form

$$(U, V) = \sum_{n=0}^{\infty} (U_n(y, t), V_n(y, t)) \Phi^{\frac{n}{3}} \exp\left[\Phi^{-\frac{11}{3}} \int_0^t \sum_{n=0}^{\infty} \sigma_n(t) \Phi^{\frac{n}{3}} dt\right] \tag{3.8}$$

with $U_1 = V_1 = \sigma_1 = 0$.

The systems to determine σ_0, σ_2 are then found to be

$$\sigma_0 U_0 = 2 \sin t V_0 B, \quad \sigma_0 V_0 = -2 \sin t U_0 B; \tag{3.9}$$

$$\left. \begin{aligned} \sigma_0 U_2 &= 2 \sin t V_2 B - \sigma_2 U_0, \\ \sigma_0 V_2 &= -2 \sin t U_2 B - \sigma_2 V_0 + \sigma_0 V_{0yy} / K^2. \end{aligned} \right\} \tag{3.10}$$

The consistency of (3.9) requires

$$\sigma_0^2 = -4 \sin^2 t B^2 \tag{3.11}$$

so that σ_0 is purely imaginary and then (3.10) has a solution if

$$V_{0yy} - \frac{K^2 \sigma_2}{\sigma_0} V_0 = 0,$$

and the solution of this equation which vanishes at $y = \pm \frac{1}{2}$ is

$$V_0 = C(t) \sin n\pi(y + \frac{1}{2}), \tag{3.12}$$

with
$$\sigma_2/\sigma_0 = -n^2\pi^2/K^2, \quad n = 1, 2, 3, \dots, \tag{3.13}$$

and $C(t)$ a function to be determined at higher order. Thus σ_2 is also purely imaginary and indeed $\sigma_3, \sigma_4, \sigma_5$ are also imaginary. The equations to determine σ_6 are found to be

$$\begin{aligned} \sigma_0 U_6 - 2B \sin t V_6 &\equiv -[\sigma_2 U_4 + \sigma_3 U_3 + \sigma_4 U_2 + \sigma_5 U_1 + (\sigma_6 + K^2) U_0] \\ &\quad + 2B[q_1 \cos t V_3 + q_2 \sin t V_2], \\ \sigma_0 V_6 + 2B \sin t U_6 &= -[\sigma_2 V_4 + \sigma_3 V_3 + \sigma_4 V_2 + \sigma_5 V_1 + (\sigma_6 + K^2) V_0] \\ &\quad + K^{-2}[\sigma_0 V_4 + \sigma_2 V_2 + \sigma_3 V_1 + \sigma_4 V_0]_{yy}, \end{aligned} \tag{3.14}$$

where
$$q_1 = \frac{y^2}{2} - \frac{1}{24}, \quad q_2 = -\frac{1}{12} \left(y^4 - \frac{y^2}{2} + \frac{7}{240} \right). \tag{3.15}$$

If we eliminate U_0, V_0 from (3.14) we obtain a differential equation for V_4 . The appropriate boundary conditions for V_4 are obtained from an investigation of the viscous wall layers which are required at $y = \pm \frac{1}{2}$. The ‘outer’ limits of the wall-layer solutions then provide the required conditions for V_4 . After a straightforward calculation we arrive at the conditions

$$\left. \begin{aligned} V_4 &= (-)^n n\pi\sigma_0^{-\frac{1}{2}}, \quad y = \frac{1}{2}, \\ V_4 &= -n\pi\sigma_0^{-\frac{1}{2}}, \quad y = -\frac{1}{2}. \end{aligned} \right\} \tag{3.16}$$

If the equation for V_4 is to have a solution satisfying these conditions then the real part of σ_6 is given by

$$\sigma_{6r} = \frac{-2n^2\pi^2 B^{\frac{1}{2}} |\sin t|^{\frac{1}{2}}}{K^2} - K^2. \tag{3.17}$$

The amplitude function $C(t)$ is determined at higher order and is found to be singular at the instants when σ_0 vanishes. In order to find the disturbance structure at such times we consider a small time interval near, for example, $t = 0$ and define

$$T = \Phi^{-1}t. \tag{3.18}$$

This scaling is implied by (3.2a) which shows that the first and second terms in the brackets on the right-hand side of this equation are comparable whenever $\sin t \sim O(\Phi)$. We then note that (3.2) may then be written in the form

$$\left(\partial_y^2 - \frac{K^2}{\Phi^{\frac{2}{3}}} - \partial_T \right) U = \frac{-2B}{\Phi^{\frac{1}{3}}} \left\{ T + \frac{1}{12} + \frac{1}{2} \left(y - \frac{1}{2} \right) + \frac{1}{2} \left(y - \frac{1}{2} \right)^2 + \dots \right\} V, \tag{3.19a}$$

$$\left(\partial_y^2 - \frac{K^2}{\Phi^{\frac{2}{3}}} - \partial_T \right) \left(\partial_y^2 - \frac{K^2}{\Phi^{\frac{2}{3}}} \right) V = \frac{-2BK^2}{\Phi^{\frac{7}{3}}} \{ T + \dots \} U. \tag{3.19b}$$

These equations may be solved using a WKB approach to take care of the time dependence and by noting that for small values of $(y - \frac{1}{2})$ we can ignore the third and fourth terms in the bracket on the right-hand side of (3.19a). In order to balance the time derivative with terms on the right-hand side of (3.19) we must take $\partial_T = O(\Phi^{-\frac{1}{3}})$

and the y -dependence of the disturbance then shrinks to a thin layer of thickness $\Phi^{\frac{2}{3}}$ near $y = \frac{1}{2}$. In fact a similar layer exists near $y = -\frac{1}{2}$ but the structure is similar to that at the upper wall. We define $\xi = (y - \frac{1}{2}) \Phi^{-\frac{2}{3}}$ and then look for a solution of (3.19) near $y = \frac{1}{2}$ of the form

$$(U, V) = [(U_0(\xi, T), V_0(\xi, T) + \Phi^{\frac{2}{3}}(U_1(\xi, T), V_1(\xi, T)) \dots] \times \exp \left[\frac{1}{\Phi^{\frac{5}{3}}} \int^T (J_0(T) + \Phi^{\frac{2}{3}} J_1(T) + \dots) dT \right]. \tag{3.20}$$

If we substitute the above expansions into (3.19) and equate terms of the powers in $\Phi^{\frac{2}{3}}$ we obtain at zeroth order a pair of linear equations for U_0, V_0 . The consistency of these equations yields

$$J_0^2 = -4B^2 T(T + \frac{1}{12}) \tag{3.21}$$

so that we have an exponentially growing solution in

$$-\frac{1}{12} < T < 0.$$

We assume that T is in this range and consider the root of (3.21) with $J_0 > 0$. At next order we find that the linear equations for U_1, V_1 obtained are consistent if

$$\frac{d^2 V_0}{d\xi^2} - \frac{2J_1}{J_0} K^2 V_0 + \frac{12K^2 \xi}{12T+1} V_0 = 0 \tag{3.22}$$

This equation is then solved subject to $V_0 = 0, \xi = 0$ and such that $V_0 \rightarrow 0, \xi \rightarrow -\infty$. This enables us to express V_0 in terms of solutions of Airy's equation and the quantity J_1 can then be expressed in terms of the zeros of A_i . The solution (3.22) fails when $T = 0, T = -\frac{1}{12}$ and WKB turning point layers (with respect to t) are needed to connect (3.8) and (3.22). Across these layers the two oscillating solutions (3.8) with $\sigma_0 = \pm 2iB \sin t$ connect with the exponentially decaying growing solutions (3.20) with $J_0 = \pm 2B[-T]^{\frac{1}{2}}(T + \frac{1}{12})^{\frac{1}{2}}$. A periodic solution is obtained by choosing B such that the exponential growth in $-\frac{1}{12} < T < 0$ cancels the exponential decay associated with σ_6 in (3.8). We note here that the particular form of the time dependence of (3.9) enables us to consider only the interval $0 < t < \pi$. If we then consider the least-decaying solution (3.17) with $n = 1$ we find that the smallest value of B that leads to a neutral solution of (3.9) for $\Phi \ll 1$ satisfies

$$\frac{2\pi^2 B^{\frac{1}{2}}}{K^2} \int_{\sigma}^{\pi} |\sin t|^{\frac{1}{2}} dt + K^2 \pi = 2B \int_{-\frac{1}{12}}^0 [-T(T + \frac{1}{12})]^{\frac{1}{2}} dT. \tag{3.23}$$

The above equation can then be solved for $B^{\frac{1}{2}}$ (implicitly assumed to be positive in the derivation of (3.23)) as a function of K . Figure 1 shows B as a function of K ; we see that $B \sim K^{-2}, B \sim K^4$, for small and large K respectively and that B attains a minimum at some intermediate value of K .

If the integral on the left-hand side of (3.23) is integrated numerically we find that the minimum occurs when

$$B = 73630, \quad K = 7.99. \tag{3.24a, b}$$

Thus the most dangerous mode for $\Phi \ll 1$ has α given by

$$\alpha = 73630 \Phi^{-\frac{11}{3}} + \dots \tag{3.25}$$

We postpone further discussion of (3.25) until the next section where we discuss the numerical solution of the eigenvalue problem for $\Phi = O(1)$.

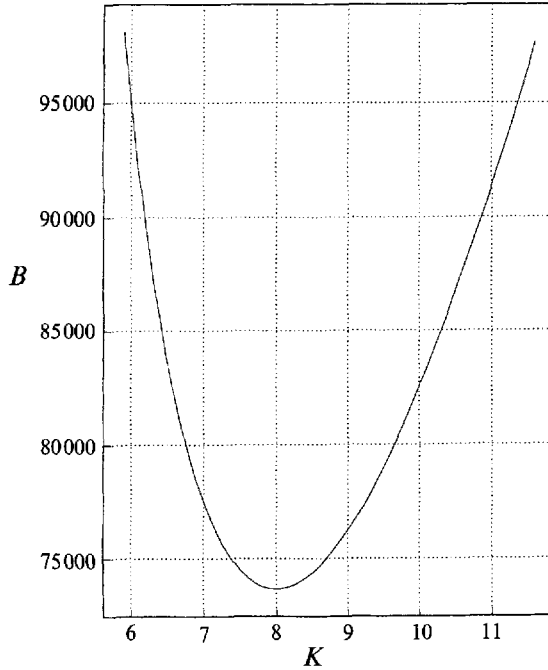


FIGURE 1. B as a function of K .

3.2. *The high-frequency limit*

For large values of the frequency parameter Φ the function $Q(y)$ appearing in the stability equations (3.1) develops boundary layers of thickness $\Phi^{-1/2}$ at $y = \pm \frac{1}{2}$ and is exponentially small elsewhere. It follows that any instability must be localized in these layers so for definiteness we focus on the layer at $y = -\frac{1}{2}$ and define

$$\eta = \Phi^{1/2}(y + \frac{1}{2}). \tag{3.26}$$

The dominant terms on the right- and left-hand sides of (3.1) then balance for $\eta = O(1)$ if

$$U \sim \alpha V \Phi^{1/2}, \quad V \sim \alpha U$$

with $k \sim O(\Phi^{1/2})$. Hence we must take $\alpha \sim \Phi^{-1/2}$ and write

$$\alpha = \frac{B}{\Phi^{1/2}} + \dots, \quad k = \hat{k} \Phi^{1/2} + \dots,$$

and the zeroth-order approximation to (3.1) in the lower wall layer can be written in the form

$$\left. \begin{aligned} (\partial_\eta^2 - \hat{k}^2 - \partial_t) U &= V \{ [(i-1)/\sqrt{2}] e^{i\frac{1}{2}\eta + it} + \text{complex conjugate} \}, \\ (\partial_\eta^2 - \hat{k}^2 - \partial_t) (\partial_\eta^2 - \hat{k}^2) V &= -2B\hat{k}^2 \sin tU, \\ U = V = V_\eta = 0, \quad \eta = 0, \quad U, V \rightarrow 0, \quad \eta \rightarrow \infty. \end{aligned} \right\} \tag{3.27}$$

Solutions of this system of the form

$$(U, V) = e^{\mu t} (\hat{U}(\eta, t), \hat{V}(\eta, t))$$

can be found and the Floquet exponent μ is then a function of B and \hat{k} . Neutral solutions then correspond to $\mu_r = 0$ and the corresponding values of \hat{k} , B are the

neutral values of the neutral wavenumber and angular displacement. In fact (3.27) is quite similar to the eigenvalue problem solved by Seminara & Hall (1976). The latter authors were concerned with the stability of the flow around a torsionally oscillating cylinder. The eigenvalue value problem $\mu = \mu(\hat{k}, B)$ associated with (3.26) is identical to that governing the stability of a vertically oscillating Boussinesq fluid of Prandtl number unity subject to a time-periodic temperature heating at the wall. If the vertical oscillations are replaced by a steady gravitational field then we obtain the eigenvalue problem discussed by Hall (1985). It is of interest to note that in that case the growing modes correspond to subharmonic disturbances.

A numerical investigation of the eigenvalue problem (3.27) showed that the only growing disturbances have $\mu_i = 0$ so that the disturbed flow is synchronous with the basic flow. Our calculations showed that the minimum value of B is given by $B = 2.9$ so that at high frequencies the boundary between stability and instability is given by

$$\alpha = 2.9\Phi^{-\frac{1}{3}} + \dots \quad (3.28)$$

We postpone a comparison of the low and high frequency predictions found above to the numerical solutions of (3.1) until the next section.

4. Numerical solutions of the eigenvalue problem for $\Phi = O(1)$

On the basis of Floquet theory we anticipate that solutions of (3.1) may be found in the form

$$(U, V) = \sum_{-\infty}^{\infty} \{U_n(y), V_n(y)\} e^{int + \mu t} \quad (4.1)$$

and the sign of μ_r , the Floquet exponent, then determines the stability characteristics of the flow in question. We obtained values of μ by substituting for (U, V) from (4.1) into (3.1) and solving the infinite set of coupled ordinary differential equations obtained by equating like powers of e^{it} by a shooting procedure. Because of the symmetries of the basic state it is possible to show that the possible eigenfunctions $(U_n(y), V_n(y))$ are either odd or even functions of y . This result was used to reduce the interval over which these functions must be calculated to $[0, \frac{1}{2}]$. However, note that all the results we obtained correspond to even modes in y and the corresponding Floquet exponent was found to be purely real. The latter result means that the disturbances are synchronous with the basic state; we note here that BM found no experimental evidence of subharmonic instabilities. Finally, before presenting our results we note that the number of Fourier terms used in the truncated form of (4.1) and the number of grid points in the Runge–Kutta integration scheme were varied until convergence was achieved. The results given here correspond to a Runge–Kutta step length 10^{-3} and 32 Fourier modes.

In figure 2 we show a sequence of neutral curves in the (k, Φ) -plane for several values of α . We see that there is a minimum value of Φ on each neutral curve, and above these curves exponentially growing modes exist. If α is varied we can compute the (α, Φ) -locus of the most dangerous mode. This curve is shown in figure 3 and is labelled $T1$. In this figure we also show some of the experimental results of BM. A detailed explanation of the experimental results shown in figure 2 can be found in the accompanying paper BM.

It appears that the theoretical curve $T1$ predicts the onset of the strong roll cells associated with II. Despite an exhaustive search we could not find any amplifying modes corresponding to the weak roll onset observed experimentally. We note here

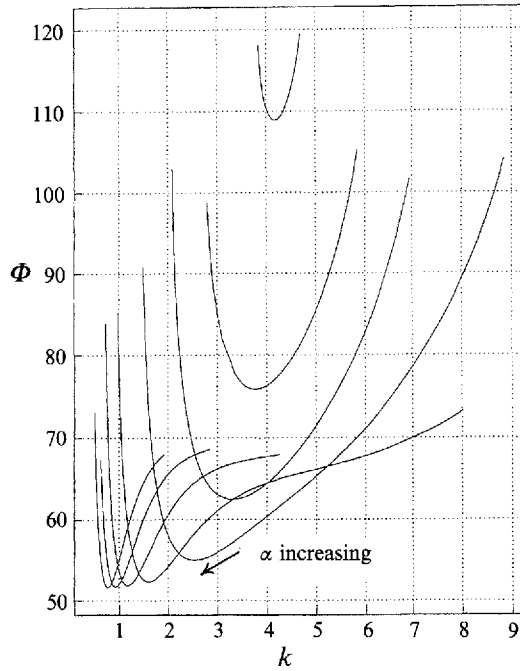


FIGURE 2. The neutral curves associated with (3.1) for $\alpha = 1.1, 1.25, 1.5, 2, 3, 4, 5, 6$.

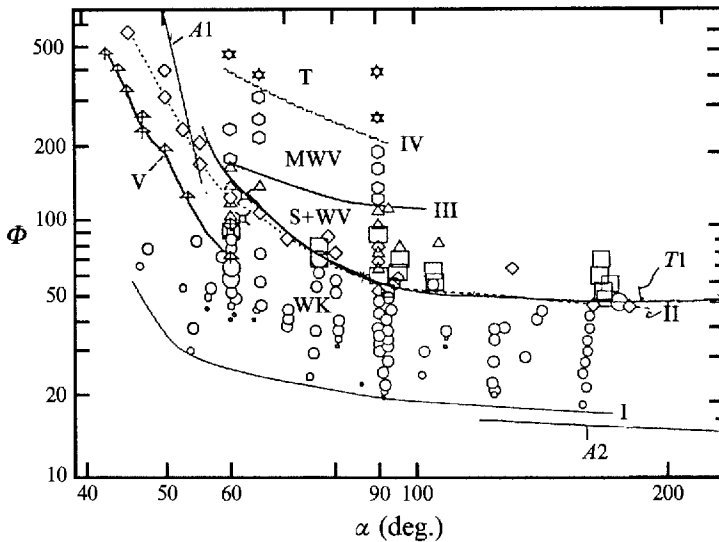


FIGURE 3. The experimental results of BM and the theoretical neutral curve ($T1$). For an explanation of the symbols used see the text of this paper and BM. The low- and high-frequency predictions are denoted by $A1$, $A2$.

that no particular time dependence of the perturbation was imposed in our calculations so that if subharmonic or superharmonic modes were unstable they would have been captured by the numerical scheme. We speculate then that the curve I of BM is associated with end effects in the experiment; certainly the fact that BM state that the roll amplitude does not increase significantly until II is crossed would tend to support this conclusion.

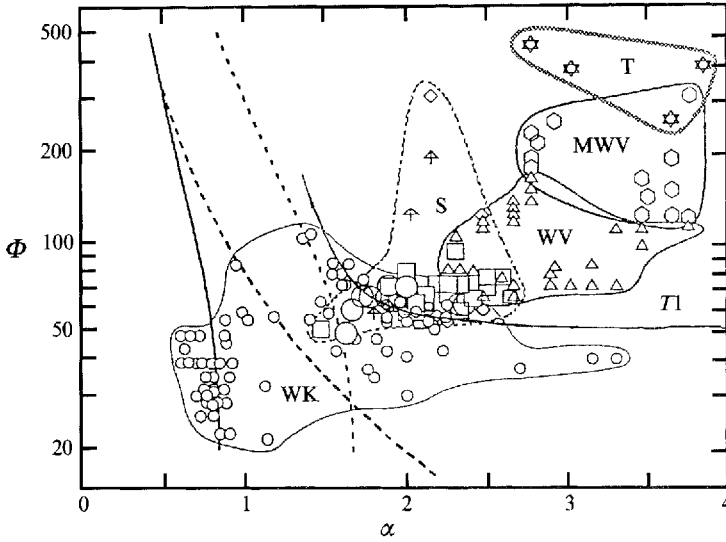


FIGURE 4. The experimental results of BM and the theoretical neutral curve (*T1*). For an explanation of the symbols used see the text of this paper and BM.

In figure 4 we compare the critical wavenumbers of our theoretical predictions with the observations of BM. We see that the onset of the strong roll state again correlates well with the theoretical work.

Finally we note that the most dangerous modes predicted by the asymptotic theories for $\Phi \gg 1$, $\Phi \ll 1$ are denoted by the curves *A1* and *A2* respectively in figure 3. We see that the high-frequency prediction agrees well with the finite- Φ calculation whilst the small- Φ prediction is not particularly accurate at the largest value of α used. However since the latter theory is based on $\alpha \gg 1$ and we have computed only for $\alpha \lesssim 3$ we presume that the difference is because the asymptotic regime has not yet been achieved. Indeed when $\alpha \sim 3$ the curve *T1* has $\Phi \sim 50$ which means that the unsteady boundary layer has a thickness of about $\frac{1}{3}d$; thus the quasi-steady response of the basic state is not yet operational.

In figure 5(*a-c*) we show the first few Fourier modes of U, V for the most dangerous mode at $\alpha = 1.1, 1.5,$ and 5 . Note that these functions are even about $y = 0$ and that u_n, v_{n-1} are zero when n is an even integer.

In order to see whether the wavy and turbulent states observed by BM are related to travelling wave disturbances we shall in the next section discuss the possible existence of shear flow instabilities.

5. Shear flow instabilities

Here we investigate the possibility that travelling wave disturbances are responsible for the onset of instability in the flow in a flapping rectangular tank. We restrict our attention to two-dimensional waves and therefore set $\partial_z = W = 0$ in (2.13). If the pressure is eliminated from the x and y momentum equations we find that V satisfies

$$\frac{1}{i\lambda R} \{ \partial_y^2 - \lambda^2 \}^2 V = \left\{ \bar{u} + \frac{\Phi}{i\lambda R} \partial_t \right\} \{ \partial_y^2 - \lambda^2 \} V - V \bar{u}_{yy}, \tag{5.1}$$

where we have defined the Reynolds number R by

$$R = \alpha \Phi.$$

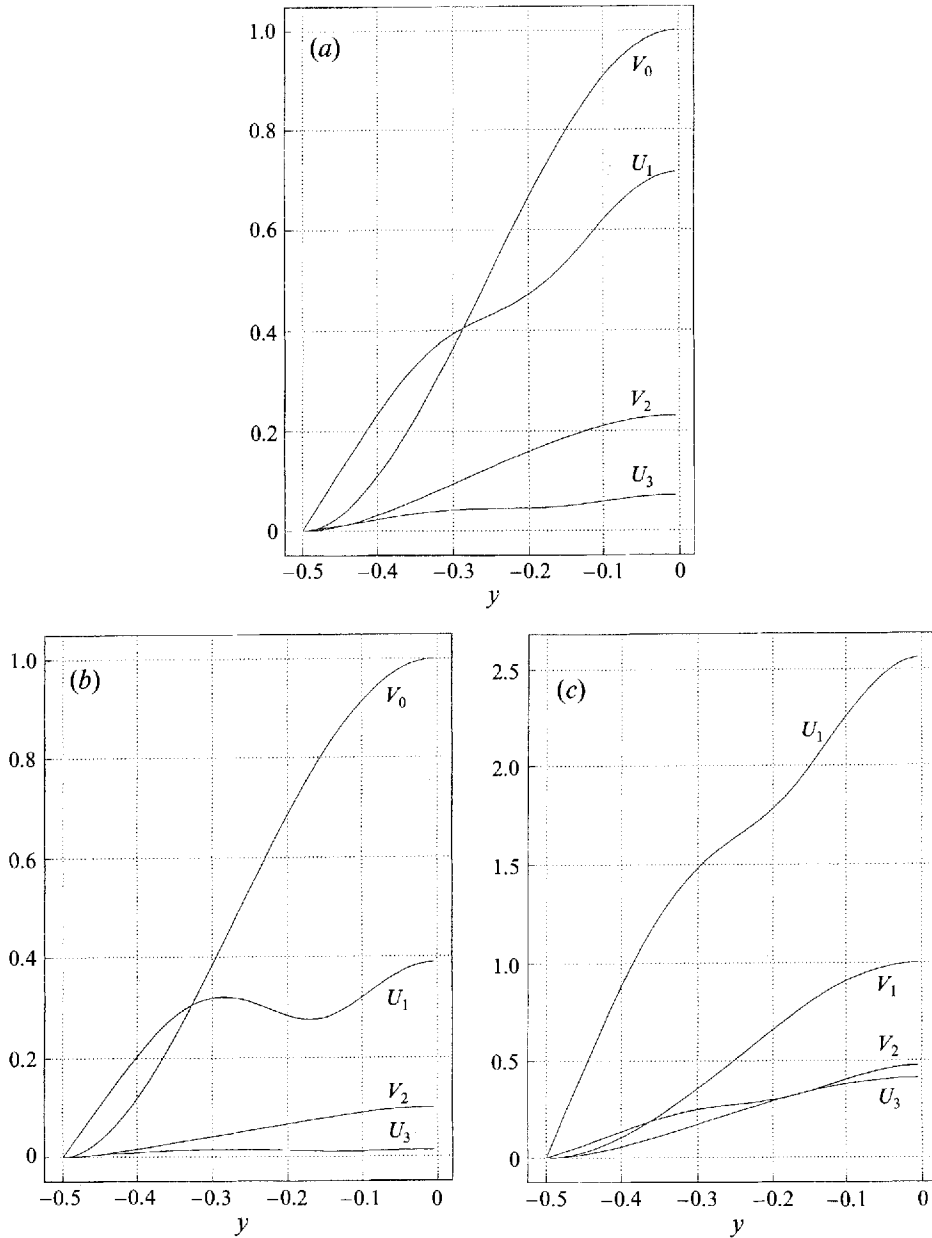


FIGURE 5. The eigenfunctions of the most dangerous modes for (a) $\alpha = 1.1$, (b) 1.5 and (c) 5. Note that u_n and v_{n-1} are zero when n is even.

We see that the terms proportional to $\sin t$ in (2.13) do not contribute to (5.1), which is therefore the generalization of the Orr–Sommerfeld equation to an unsteady parallel flow $u = \bar{u}(y, t)$.

Equation (5.1) may be solved using the approach of Hall (1978) who used Floquet theory to convert the same equation for a Stokes-layer mean flow into an infinite sequence of coupled Orr–Sommerfeld equations. Here we shall restrict our attention to solutions of (5.1) for small and large values of the frequency parameter Φ .

In the high-frequency limit we recall that \bar{u} is given by (2.10) for $(y + \frac{1}{2}) = O(\Phi^{-\frac{1}{2}})$. A

similar asymptotic form applied in the upper boundary layer so that any instability will be localized near $y = \pm \frac{1}{2}$. In fact \bar{u} given by (2.10) is exactly the Stokes-layer velocity profile for the case when the flow is driven by an oscillatory pressure gradient. Hence if we define $\eta = \Phi^{\frac{1}{2}}(y + \frac{1}{2})$ and let

$$\lambda = \Phi^{\frac{1}{2}}\hat{\lambda}, \quad R = \Phi^{\frac{1}{2}}\hat{R}$$

then (5.1) reduces to

$$\frac{1}{i\lambda\hat{R}}(\partial_\eta^2 - \hat{\lambda}^2)^2 V = \left\{ \hat{u} + \frac{1}{i\lambda\hat{R}}\partial_t \right\} \left\{ \partial_\eta^2 - \hat{\lambda}^2 \right\} V - \hat{u}_{\eta\eta} V \quad (5.2)$$

with

$$\hat{u} = \sin t - \sin [t + 2^{-\frac{1}{2}}\eta] \exp(2^{-\frac{1}{2}}\eta)$$

which is to be solved subject to

$$V = V_\eta = 0, \quad \eta = 0, \infty. \quad (5.3)$$

The partial differential system (5.2)–(5.3) is identical to that governing the instability of a Stokes layer to Tollmien–Schlichting waves; see Kerczek & Davis (1974), Hall (1978).

Thus for $k = 0$ the stability of the flow in a rectangular tank flapping at high frequencies is governed by the equations that determine the stability of a Stokes layer. The Floquet analysis of (2.14) given by Hall (1978) suggests that a Stokes layer is stable; on the other hand the quasi-steady approaches of Kerczek & Davis (1974) show that instantaneous profiles can be highly unstable because of their inflexional nature. The results of these different approaches can be reconciled by noting that the quasi-steady solutions cannot be connected to the Floquet solutions by extending them over a whole period. Nevertheless the results of the quasi-steady calculations are consistent with experimental observations and suggest instability will occur for part of the period whenever \hat{R} is greater than about 200. This suggests that at high frequencies localized shear instabilities will occur when

$$\alpha > 200\Phi^{-\frac{1}{2}}$$

whilst roll modes occur when

$$\alpha > 2.9\Phi^{-\frac{1}{4}}.$$

It follows that, in an experiment with Φ fixed, transition will probably be caused by shear instabilities waves for small enough values of α . However, α must be less than about 0.05 for the shear instabilities wave to become dominant; this regime was not investigated experimentally so it is not surprising that the asymptotic prediction given above is off the scale of figure 2.

Now let us turn to the low-frequency limit $\Phi \rightarrow 0$; in this limit \bar{u} is given by (2.11) and (5.1) may be written in the form

$$\frac{1}{i\lambda\hat{R}}\{\partial_y^2 - \lambda^2\}^2 V = \left\{ \bar{u} \cos t + \dots + \frac{\Phi}{i\lambda\hat{R}}\partial_t \right\} \{\partial_y^2 - \lambda^2\} V - \cos t \bar{u}_{yy} V + \dots = 0, \quad (5.4)$$

where

$$\bar{u} = \frac{1}{12}y\{1 - 4y^2\}, \quad \hat{R} = \Phi R. \quad (5.5)$$

Equation (5.4) is to be solved subject to the conditions that V, V_y should vanish at $y = \pm \frac{1}{2}$. The slow time variation of the basic state can be taken care of for the disturbance by a WKB approach; we therefore expand V in the form

$$V = \exp\left[\frac{-i\lambda\hat{R}}{\Phi} \int^t c(t) dt\right] [\hat{V}_0(y, t) + \Phi \hat{V}_1(y, t) + \dots]$$

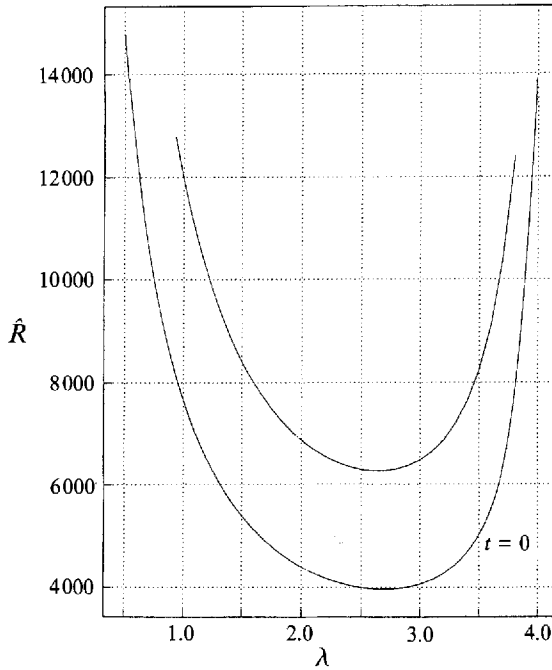


FIGURE 6. The neutral curves associated with (5.6) with $t = 0$ (lower curve) and the Floquet theory prediction.

and $c(t)$ is then determined by the instantaneous Orr–Sommerfeld eigenvalue problem

$$\left. \begin{aligned} \frac{1}{i\lambda\hat{R}} \{ \partial_y^2 - \lambda^2 \}^2 \hat{V}_0 = \{ \bar{u}(y) \cos t - c \} \{ \partial_y^2 - \lambda^2 \} \hat{V}_0 - \cos t \bar{u}_{yy} \hat{V}_0 = 0, \\ \hat{V}_0 = \hat{V}_{0y} = 0, \quad y = 0, 1. \end{aligned} \right\} \quad (5.6)$$

Thus the effective Reynolds number associated with the velocity field $\bar{u}(y)$ is $(\hat{R} \cos t)$. In figure 6 we show the neutral curve $\lambda = \lambda(\hat{R} \cos t)$ which marks the boundary between locally growing and decaying solutions. Thus whenever t and \hat{R} are such that $|\hat{R} \cos t|$ is greater than its value on the neutral curve at a fixed λ the solution is locally growing. We further note that figure 6 is the neutral curve for the shear instability of the flow in a channel rotating with a steady angular velocity. In addition it should be noted that all the eigenvalues we found had zero wave speed so that the instability wave corresponds to a standing wave instability. However large we choose \hat{R} , it will be the case that $|\hat{R} \cos t|$ is sufficiently small for the part of the cycle so that the disturbance is locally decaying. The integrated value of the growth rate over a cycle then determines the stability property of the flow according to Floquet theory. Note that it is sufficient for us to consider only half a period of the basic flow so that the neutral solutions based on Floquet theory are given by

$$\text{Im} \left\{ \int_0^\pi c(t) dt \right\} = 0, \quad (5.7)$$

where $\text{Im} \{ \}$ denotes the imaginary part of a complex quantity. In figure 6 we also show the neutral curve obtained by the imposition of this condition. We see that instability occurs for $\hat{R} > 3965$ and unstable modes occur over a finite range of values of the wavenumber λ . The fact that the band of unstable wavenumbers is finite is a direct

consequence of the fact that \bar{u} has an inflexion point so that at any instant in time when $\cos t \neq 0$ at sufficiently high values of \hat{R} the instantaneous neutral problem has a mode with $c_r = 0$. Finally we note that our calculations predict the onset of shear instabilities when

$$\alpha > 3965\Phi^{-2}. \quad (5.8)$$

The unstable region predicted by (5.8) is off the scale in figure 3 so it would appear that the wavy and turbulent regimes in BM are not associated with shear instabilities. However, it should be remembered that (5.8) is valid only for $\Phi \ll 1$; at $O(1)$ values of the frequency parameter the stability of the basic state can only be determined by solving (5.1) numerically. We do not pursue that calculation here since our asymptotic results suggest that shear instabilities are not important in the experimental range investigated by BM. Nevertheless the Floquet solutions of (5.1) are of some interest since we know that at small values of Φ unstable solutions exist whilst at large Φ equation (5.1) governs the instability of a Stokes layer. Since no unstable Floquet solutions have ever been obtained for the latter problem it will be of interest to determine where the small- Φ unstable solutions become stabilized at larger Φ .

6. Conclusions

Our investigation has shown that the flow in an oscillating fluid tank is susceptible to at least two types of instability. The first mode is the roll mode having cell boundaries parallel to the (x, y) -plane whilst the other instability, the wave mode, is periodic in the x -direction. Furthermore, in the low-frequency limit the wave mode is stationary so that the instability takes the form of rolls which are now parallel to the (y, z) -plane. The onset of the strong mode observed by BM is explained by the most dangerous linear disturbance discussed in §4 of this paper. We suspect that the weak roll observed by BM is a manifestation of end effects in their apparatus and is therefore not accessible to a linear instability analysis. The roll modes we have discussed have a close relationship with centrifugal and convective instabilities in time-periodic boundary layers and it is of interest to determine the destabilizing mechanism in the present situation. In fact we see in (3.1) that the terms on the right-hand side of the V -equation, which are responsible for the instability, arise from the Coriolis terms in the Navier–Stokes equation written in the rotating frame. Thus the roll mode is produced by Coriolis effects. On the other hand the wave mode is associated with an inflexion-point instability in both the high- and low-frequency limits. More precisely the wave instability discussed in §5 at small values of Φ is an inviscid instability associated with the inflexional velocity profile $\bar{u}(y)$. Our calculations suggest that, at low frequencies, this mode does not play a significant role in the highly nonlinear stages investigated experimentally by BM. However, the wave instability might be more unstable at finite values of the frequency parameter. This possibility has not been investigated numerically but certainly the results of BM suggest this as a strong possibility. However, as pointed out to the author by Professor Bolton, the wavy mode might simply be an instability of the nonlinear rolls. At high frequencies the wave mode is a locally unstable Stokes-layer instability. BM do not give any results that suggest that this instability is present in their experiments. We note that this is a highly localized mode and so if it were present in the experiments it would almost certainly be detected.

In addition to the higher-order linear roll mode and travelling wave disturbances there are other candidates for the secondary and tertiary instabilities observed in the experiments. We refer to the inviscid modes induced by finite-amplitude vortices in

boundary-layer flows. These modes, which were discussed by Hall & Horseman (1991), arise when a finite-amplitude vortex modifies the underlying boundary layer so as to make it unstable to Rayleigh waves. The secondary instability in that problem tends to be created at particular spanwise locations but there is no suggestion that this type of localization occurs in the flapping tank problem.

The author acknowledges some useful conversations with Professor R. E. Kelly in connection with this work.

This research was partially supported by the National Aeronautics and Space Administration under NASA Contract No. NAS1-18605 while the author was in residence at the Institute for Computer Applications in Science and Engineering (ICASE), NASA Langley Research Center, Hampton, VA 23665. This work was also supported by SERC.

REFERENCES

- AKHAVAN, R., KAMM, R. D. & SHAPIRO, A. H. 1991*a* An investigation of transition to turbulence in bounded oscillatory Stokes flows. Part 1. Experiments. *J. Fluid Mech.* **225**, 395–422.
- AKHAVAN, R., KAMM, R. D. & SHAPIRO, A. H. 1991*b* An investigation of transition to turbulence in bounded oscillatory Stokes flows. Part 2. Numerical simulations. *J. Fluid Mech.* **225**, 423–444.
- BOLTON, E. W. & MAURER, J. 1994 A new roll type instability in an oscillating fluid plane. *J. Fluid Mech.* **268**, 293–313 (referred to herein as BM).
- GRESHO, P. M. & SANI, R. L. 1970 The effects of gravity modulation on the stability of a heated fluid layer. *J. Fluid Mech.* **40**, 783–806.
- HALL, P. 1978 The linear stability of flat Stokes layers. *Proc. R. Soc. Lond. A* **359**, 151–166.
- HALL, P. 1981 Centrifugal instability of a Stokes layer: subharmonic destabilization of the Taylor vortex mode. *J. Fluid Mech.* **105**, 523–530.
- HALL, P. 1984 On the stability of the unsteady boundary layer on a cylinder oscillating transversely in a viscous fluid. *J. Fluid Mech.* **146**, 347–367.
- HALL, P. 1985 On the instability of time-periodic flows. In *Instability of Spatially and Temporally Varying Flows* (ed. M. Hussaini & P. Vogt), pp. 206–224. Springer.
- HALL, P. & HORSEMAN, N. J. 1991 The inviscid secondary instability of fully nonlinear vortex structures in growing boundary layers. *J. Fluid Mech.* **232**, 357–375.
- KERCZEK, C. VON & DAVIS, S. H. 1974 Linear stability theory of oscillatory Stokes layers. *J. Fluid Mech.* **62**, 753–773.
- PAPAGEORGIOU, D. 1987 Stability of unsteady viscous flow in a curved pipe. *J. Fluid Mech.* **182**, 209–233.
- PARK, K., BARENGHI, C. & DONNELLY, R. J. 1980 Subharmonic destabilization of Taylor vortices near an oscillating cylinder. *Phys. Lett.* **78A**, 152–154.
- SEMINARA, G. & HALL, P. 1976 Centrifugal instability of a Stokes layer: linear theory. *Proc. R. Soc. Lond. A* **350**, 299–316.